Reliability and performance evaluation of retrial repairable systems with an unreliable repairer using the $GSPN$ model

Kheireddine Boudehane [1,*] and Samira Taleb [1]

[1] *Department of Probability and Statistics, Faculty of Mathematics, RIIMA Laboratory, University of Science and Technology Houari Boumediene, B.P. 32, 16111, Algiers, Algeria*
E-mail: kboudehane@usthb.dz, staleb@usthb.dz

Abstract. Generalized Stochastic Petri Nets ($GSPNs$) are widely used in reliability analysis to model and optimize the dependability of complex systems, enabling assessments of availability, failure probabilities, and repair processes through stochastic timing. This study investigates a repairable redundant retrial system incorporating warm and cold standbys and an unreliable repairer through a Generalized Stochastic Petri Nets. The repairer experiences both active (during repair) and passive (idle) breakdowns. Component and repairer lifetimes are exponentially distributed. A component that fails undergoes immediate repair if the repairer is available; otherwise, it enters a retrial $FCFS$ orbit. A Continuous Time Markov Chain ($CTMC$) derived from the $GSPN$ model yields steady state probabilities and availability. System reliability and time to first failure are then determined via Laplace transforms. Numerical examples demonstrate the system reliability performance.

Keywords: K-out-of-n : G system, reliability, generalized stochastic Petri net, standby redundancy

Received: March 2, 2025; accepted: July 26, 2025; available online: December 23, 2025

DOI: 10.17535/crorr.2026.0010

Original scientific paper.

1. Introduction

Reliability engineering focuses on designing and developing systems for consistent performance throughout their operational life with minimal probability of failure. It encompasses various methodologies, including failure analysis, risk assessment, and redundancy techniques, to ensure systems meet their reliability targets. A K-out-of-n : G system is deemed successful if a minimum of K units remain operational among the n components. These systems are frequently employed in fault-tolerant designs, where the objective is to maintain system functionality despite component failures. By incorporating redundancy, K-out-of-n systems help achieve this goal.

Standby redundancy enhances system reliability by having backup components that can seamlessly replace failed primary components. This redundancy is categorized as hot (backups continuously active), warm (pre-configured backups with minimal activation delay), or cold (inactive backups requiring manual initiation upon primary component failure). Hot standby components share the same failure rate with primary components, standby mode, failure rate of cold components is zero, while warm components failure rate is between the two. Readers interested in the topic are encouraged to refer to Barlow and Proshan [3], Birolini [4], David [20], Lai and Xie [17] and Kececioglu [15].

Our understanding of standby redundancy and K-out-of-n systems has been significantly advanced through numerous studies exploring reliability analysis, system configurations, and

*Corresponding author.

maintenance strategies. For example, Srinivas et al. [21] studied the system reliability under the (N, T) policy. The reliability of generalized repairable systems incorporating cold and warm components in standby are explored by Wang and Loman [24] and Ke and Wang [13] respectively. Yuan [25] examined availability and reliability in systems with multiple vacations. Other studies, such as, Amari [1] and Levitin and Amari [18], focused on reliability algorithms and failure time distributions for systems incorporating shared units in standby. Systems with retrial phenomena have been explored by Ke et al. [14] and Kuo et al. [16]. Bounds for reliabilities under probabilistic constraints are derived by Unuvar et al. [22]. In [12] a warm standby system is studied using the semi Markov process and regenerative point technique.

Generalized Stochastic Petri Nets ($GSPNs$) are bipartite graphs having the power to model complicated systems. They also describe and analyze stochastic concurrent systems with synchronization properties. They extend the capabilities of the classical Petri nets by using probabilities to represent the timing of events in complex systems. Graphically, a $GSPN$ consists of places (circles), tokens (black dots or numbers), and transitions. Transitions are of two types: immediate transitions (thin bars), which fire instantaneously, and timed transitions (rectangles), which have an exponentially distributed duration. Arcs connect transitions and places, indicating the circulation of tokens. Transitions are prevented from firing by inhibitor arcs. Timed transitions lead to tangible markings, while immediate transitions result in vanishing markings. A reachability graph shows all possible states (markings) of a $GSPN$, with nodes representing markings and edges representing transition firings. A $CTMC$ is isomorphic to $GSPN$ tangible reachability graph. A $GSPN$ has a steady-state probability distribution if its initial marking represents a home state (the system can return to it from any other marking) and it is bounded (has finite tokens in each place). $GSPNs$ are successfully used to model manufacturing systems [2, 23], computer science [6, 8, 28], business processes [5], queuing systems [7, 9, 10], and wireless networks [26, 27]. Besides these applications, $GSPNs$ are also widely used in reliability analysis of systems, providing powerful tools for modeling and evaluating system performance and dependability [30, 27, 11, 29]

The aim of our work is to examine a retrial K-out-of-n:G system incorporating warm and cold components in standby with an unreliable repairer using a Generalized Stochastic Petri Net.

The following is the paper's structure: Section 2 describes the K-out-of-n system incorporating warm and cold standbys and an unreliable repairer and presents the proposed $GSPN$ model. Section 3 delves into both steady-state and transient analysis, deriving key reliability indices system availability, reliability function, and the mean time to first failure ($MTTF$). Section 4 concludes with comprehensive illustrative examples that examine the influence of system variables on the reliability indices.

2. Model Description

We investigate a retrial K-out-of-$n : G$ system, composed of M uniform primary operational components, supported by W warm and C cold components in standby. The system operates as long as at least K components (out of the total $M + W + C$) are in operational mode (either actively operating or available in standby). The system units are prone to failure, and any failed component is repairable. Upon failure of a primary operating component, immediate replacement occurs using an available warm standby component, if one exists; otherwise, a cold standby component is activated as the new primary component. Similarly, if a warm standby component fails while it is on standby, it will be replaced immediately by an available cold component. Repairer failures can occur during active repair periods (active breakdowns) and during periods of inactivity (passive breakdowns). Upon failure, a component joins an $FCFS$ orbit for a random duration if the repairer is either undergoing repair or busy.

We assume that:

- Failures of primary and warm units are characterized by Poisson processes, with rates η and α ($\eta > \alpha > 0$) respectively,
- Upon failure, a unit is immediately repaired if the repairer is available.An exponential distribution with mean $\frac{1}{\mu}$ governs the repair times of all components,
- The repairer is subject to Poisson failures with rate δ when busy and θ when idle. The repairer recovery time is characterized by an exponential distribution with parameter σ,
- If the repairer is unavailable (busy or under repair), failed components join an $FCFS$ orbit. Subsequently, the repairer selects the next component from the orbit for service, with the selection time following an exponential distribution with mean $\frac{1}{\gamma}$,
- All stochastic processes are assumed to be independent.

2.1. Practical example

Underground mining operations generate significant amounts of toxic and dangerous gases, which not only have harmful effects on the personal safety and health of employees, but also force severe halts to mining activities. The mine must have complete and autonomous ventilation equipment, or mine ventilators, to provide adequate fresh air underground and to diffuse and remove dangerous and poisonous gases. Assume that this ventilation system has M working mine ventilators, W warm standby ventilators, and C cold standby ventilators. At least K ventilators must be operational to ensure the purity of underground air. If $M+W+C-K+1$ mine ventilators fail, the ventilation system fails. We assume that all mine ventilators are new at time $t=0$. Operating and warm mine ventilators fail independently of each other. An available warm ventilator (or an available cold one) replaces a failed operating mine ventilator (or a failed warm one). When a failed mine ventilator finds the repairer available, it is repaired immediately and restored to perfect condition. Mine ventilators may experience breakdowns during either the repair service period or idle periods due to malfunctions or lifetime limitations and need to be repaired. Upon failure, a component is placed in a buffer (referred to as an orbit) and waits there if the repairer is busy or out of order. Once available, the repairer selects one of the failed mine ventilators from the orbit queue, if any are present. Consequently, a ventilation safety system with an unreliable repairer can be modeled as a retrial repairable system incorporating warm and cold standby components and an unreliable repairer.

2.2. *GSPN* description

Figure 1 depicts the $GSPN$ model of our retrial K-out-of-n system, incorporating warm and cold standbys and an unreliable repairer. The Places of the $GSPN$ are defined as the following:

- Primary operating components, Warm standby components and cold standby components are represented by places P_M, P_W and P_C with an initial marking of M, W and C receptively,
- Place S indicates whether a failed component, either newly failed or selected from the orbit, is ready for repair,
- The orbit is represented by place *Orbit*,
- Components under repair are represented by place *Rep*,

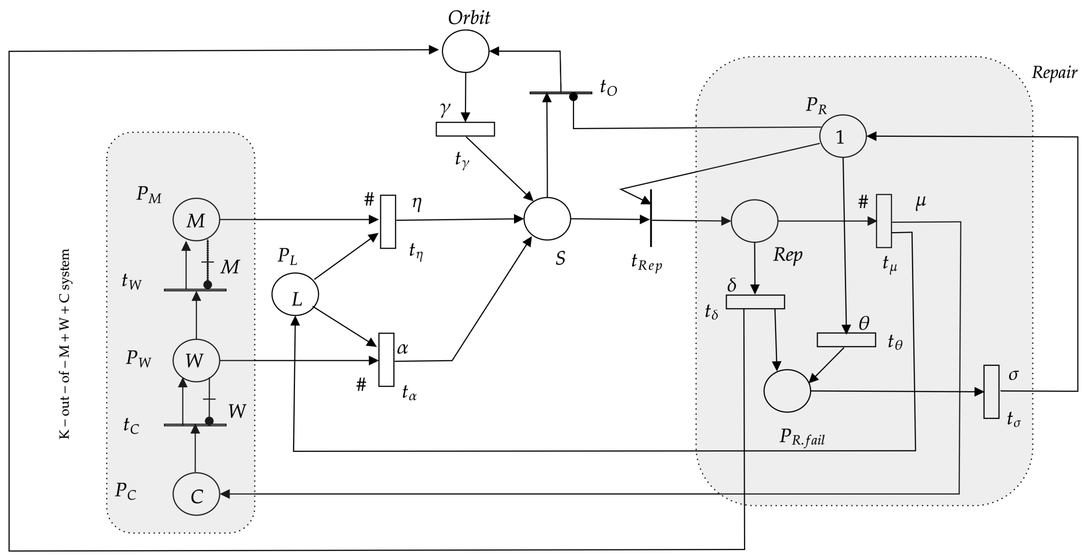

Figure 1: *GSPN model for the retrial K-out-of-n : G system incorporating warm and cold standbys and a single unreliable repairer*

- Failed repairer is represented by place $P_{R.fail}$. This place signifies that the repairer is unavailable due to a failure,

- Free repairer is represented by place P_R. This place indicates that the repairer is operational and ready to address component failures,

- Number of failed components: represented by place $P_L(L = M + W + C - K + 1)$. This place tracks the current number of components requiring repair.

Thus, the $GSPN$ starts with an initial marking M_0, which is:

$$M_0(\#P_M, \#P_W, \#P_C, \#P_L, \#Orbit, \#P_R, \#S, \#Rep, \#P_{fail}) = M_0(M, W, C, L, 0, 1, 0, 0, 0),$$

where # refers to the marking of a place p.

The failure of a primary or a warm component is modeled by the firing of transitions t_η and t_α with rates $\#P_M\eta$ and $\#P_W\alpha$ respectively. The arrival of a selected component from the orbit is characterized by the firing of transition t_γ with rate γ. The end of the repair period is represented by the firing of transition t_μ with rate μ. Active and passive breakdowns of the repairer are represented by the firing of transitions t_δ and t_θ with rates δ and θ respectively. The recovery period for the failed repairer is characterized by the firing of transition t_σ with rate σ. Transition t_{Rep} fires when place S contains one token (indicating a component ready for repair) and the repairer is available (P_R has a token). Transition t_O (indicates that the failed component is placed in orbit) fires if the repairer is under repair or busy. Transition t_W fires if P_M has fewer tokens than M (replacing a failed primary component with a warm component). Transition T_C fires if P_W has fewer tokens than W (replacing a failed warm component with a cold component). The place P_L tracks failed components, and when L components fail (resulting in P_L having 0 tokens), transitions t_η and t_α are disabled, indicating the retrial K-out-of-$n : G$ system incorporating warm and cold standbys and an unreliable repairer failure.

The set of places, transitions, and inhibitor arcs that define the structure and behavior of the Petri net model are formally presented in Tables 1, 2, and 3.

Place	Description
P_M	Represents primary operating components, initialized with M tokens.
P_W	Represents warm standby components, initialized with W tokens.
P_C	Represents cold standby components, initialized with C tokens.
S	Indicates whether a failed component (newly failed or selected from the orbit) is ready for repair.
Orbit	Represents the orbit where failed components wait to be selected for repair.
Rep	Represents components currently under repair.
$P_{R.fail}$	Signifies the failed state of the repairer (i.e., the repairer is unavailable due to failure).
P_R	Indicates a free and operational repairer ready to address component failures.
P_L	Tracks the number of failed components; $L = M + W + C - K + 1$.

Table 1: *Description of Places in the GSPN Model*

From Place	To Transition (Immediate)	Role of the Inhibitor Arc
P_M	t_W	Prevents the firing of t_W when $\#P_M = M$
P_W	t_C	Prevents the firing of t_C when $\#P_W = W$
P_R	t_O	Prevents the firing of t_O when $\#P_R = 1$

Table 2: *Inhibitor arcs and their roles (transition-focused)*

Transition	Type	Description	Firing time/rate
t_η	Timed	Failure of a primary component	Rate: $\#P_M\eta$
t_α	Timed	Failure of a warm standby component	Rate: $\#P_W\alpha$
t_γ	Timed	Selected component arrival from orbit	Rate: γ
t_μ	Timed	Completion of repair process	Rate: μ
t_δ	Timed	Active breakdown of the repairer	Rate: δ
t_θ	Timed	Passive breakdown of the repairer	Rate: θ
t_σ	Timed	Recovery of failed repairer	Rate: σ
t_{Rep}	Immediate	Repair begins if the component is ready and the repairer is free	Fires if $\#S = 1$ and $\#P_R = 1$
t_O	Immediate	Failed component routed to orbit	Fires if $\#P_{R.fail} = 1$ or $\#P_R = 0$
t_W	Immediate	Warm component replaces failed primary component	Fires if $\#P_M < M$
t_C	Immediate	Cold component replaces failed warm component	Fires if $\#P_W < W$

Table 3: *GSPN Transition Descriptions and Semantics*

3. Stochastic analysis

The goal of this section is to evaluate the steady-state and transient behavior of the retrial K-out-of-$M + W + C$ system incorporating warm and cold standbys and a single unreliable repairer and derive the main reliability indices including steady-state availability, reliability function and $MTTF$.

At time t, the marking of the system is characterized by three token counts: $F(t)$ in place *Rep*, $O(t)$ in *Orbit*, and $B(t)$ in $P_{R.fail}$. The $GSPN$ behavior is captured by the Markovian marking process $\{X(t), t \geq 0\} = \{(F(t), O(t), B(t)), t \geq 0\}$, defined on the state space $E = \{(i, j, n) : 0 \leq i \leq 1, 0 \leq j \leq L - 1, 0 \leq n \leq 1\} \cup (0, L, 0), (0, L, 1)$, with state-transition rate diagram depicted in Figure 2.

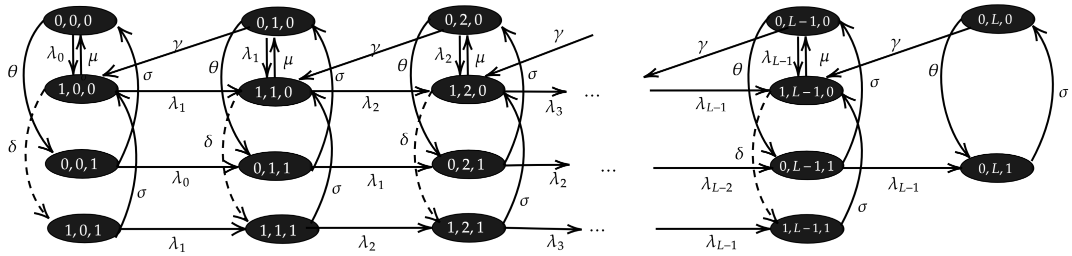

Figure 2: *State-transition diagram of the K-out-of-n;G retrial system incorporating warm and cold standbys and an unreliable repairer*

To clarify the structure of the state space and the system's dynamic behavior, we present a small-scale example with parameters $M = 2$, $W = 1$, $C = 1$, and $K = 3$, along with its corresponding reachability graph and associated $CTMC$, shown in Figures 3a and 3b, respectively

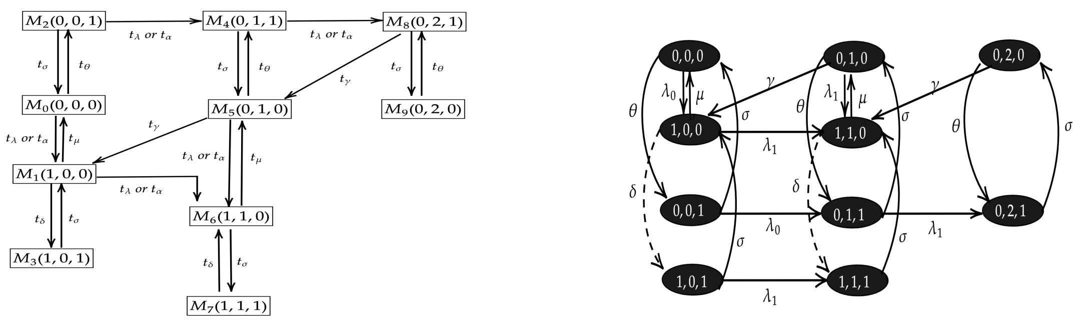

(a) *Reachability graph for the GSPN model with $M = 2$, $W = 1$, $C = 1$, and $K = 3$*

(b) *$CTMC$ representation derived from the reachability graph in Figure 3a*

Figure 3: *(a) Reachability graph and (b) its corresponding $CTMC$ for the $GSPN$ model with $M = 2$, $W = 1$, $C = 1$, and $K = 3$.*

The transition rate matrix Q of the marking process, of order $4L+2 \times 4L+2$, is a tridiagonal block matrix given as follows:

$$Q = \begin{pmatrix} B_0 & C_0 & & & & \\ A & B_1 & C_1 & & & \\ & A & B_2 & C_2 & & \\ & & \ddots & \ddots & \ddots & \\ & & & A & B_{L-1} & C_{L-1} \\ & & & & A_L & B_L \end{pmatrix}_{4L+2\times 4L+2},$$

where

$$B_0 = \begin{bmatrix} -(\eta_0+\theta) & \eta_0 & \theta & 0 \\ \mu & -(\eta_1+\mu+\delta) & 0 & \delta \\ \sigma & 0 & -(\eta_1+\sigma) & 0 \\ 0 & \sigma & 0 & -(\eta_1+\sigma) \end{bmatrix},$$

$$B_j = \begin{bmatrix} -(\eta_j+\theta+\gamma) & -\eta_j & \theta & 0 \\ \mu & -(\mu+\delta) & 0 & \delta \\ \sigma & 0 & -\sigma & 0 \\ 0 & \sigma & 0 & -\sigma \end{bmatrix}, \quad j=0,1,\ldots,L-1, \quad B_L = \begin{bmatrix} -(\theta+\gamma) & \theta \\ \sigma & -\sigma \end{bmatrix},$$

$$A = \begin{bmatrix} 0 & \gamma & 0 & 0 \\ 0 & 0 & 0 & 0 \\ 0 & 0 & 0 & 0 \\ 0 & 0 & 0 & 0 \end{bmatrix}, \quad A_L = \begin{bmatrix} 0 & \gamma & 0 & 0 \\ 0 & 0 & 0 & 0 \end{bmatrix},$$

$$C_j = \begin{bmatrix} 0 & 0 & 0 & 0 \\ \eta_{j+1} & 0 & 0 & 0 \\ 0 & \eta_j & 0 & 0 \\ 0 & 0 & \eta_{j+1} & 0 \end{bmatrix}, \quad j=0,1,\ldots,L-2, \text{and} \quad C_{L-1} = \begin{bmatrix} 0 & 0 \\ 0 & 0 \\ 0 & \eta_{L-1} \\ 0 & 0 \end{bmatrix}.$$

Given j failed units, the system instantaneous failure intensity η_j is as follows:

$$\eta_j = \begin{cases} M\eta + W\alpha, & j \in [0, C-1], \\ M\eta + (M+W-j)\alpha, & j \in [C, W+C-1], \\ (M+W+C-j)\eta, & j \in [W+C, L-1]. \end{cases}$$

3.1. Steady-State Distribution

The $GSPN$ model depicted in Figure 1 admits a steady-state probability distribution because its initial marking represents a home state and it is bounded. Let $P = (P_0, P_1, \ldots, P_{L-1}, P_L)$ be the stationary probabilities vector where $P_j = (P_{0,j,0}, P_{1,j,0}, P_{0,j,1}, P_{1,j,1})$ $(j = 0, 1, \ldots, L-1)$ and $P_L = (P_{0,L,0}, P_{0,L,1})$. The vector P satisfies the following matrix equations:

$$P_0 B_0 + P_1 A = \mathbb{O}_4, \tag{1}$$

$$P_{j-1} C_{j-1} + P_j B_j + P_{j+1} A = \mathbb{O}_4,\ j = 1, 2, \ldots, L-1, \tag{2}$$

$$P_{L-1} C_{L-1} + P_L B_L = \mathbb{O}_2, \tag{3}$$

where $\mathbb{O}_4 = (0,0,0,0)$ and $\mathbb{O}_2 = (0,0)$.

We summarize the steady-state distribution $P_j (j = 1, 2, \ldots, L)$, for the model in the following theorem:

Theorem 1. *For a retrial K-out-of-$M+W+C : G$ system incorporating warm and cold standbys and an unreliable repairer with state space E, the steady-state probabilities $P_j, (j = 1, 2, \ldots, L)$ are as follows*

$$P_0 = P_{0,0,0} r_0, \tag{4}$$

$$P_{0,0,0} = \frac{1}{r_0((\mathbb{I}_4 + \sum_{j=1}^{L} \prod_{m=0}^{j-1} R_i) e_4 + R_L e_2))} \quad , \tag{5}$$

$$P_j = P_0 \prod_{i=0}^{j-1} R_i,\ j = 1, 2, \ldots, L, \tag{6}$$

and

$$P_L = P_{L-1} R_L \tag{7}$$

where $R_n = -C_n(B_{n+1} + R_{n+1}A)^{-1}$, $R_L = -C_{L-1}B_L^{-1}$, $\mathbb{I}_4$ *is the identity matrix,*

$e_2 = \begin{bmatrix}1\\1\end{bmatrix}$, $e_4 = \begin{bmatrix}1\\1\\1\\1\end{bmatrix}$ *and* $r_0 = (1, \frac{\eta_0}{\mu} + \frac{\theta\eta_1}{\mu(\eta_1+\sigma)}, \frac{\theta}{(\eta_1+\sigma)}, \frac{\delta}{(\eta_1+\sigma)}(\frac{\eta_0}{\mu} + \frac{\theta\eta_1}{\mu(\eta_1+\sigma)}))$.

Proof. Using equations (1)-(3) together with $\sum_{j=0}^{L-1} P_n e_4 + P_L e_2 = 1$, the result is derived through straightforward calculations and substitutions. □

Let A_∞ denote the steady-state availability, representing the steady-state probability of system operability. Hence, we have

$$A_\infty = 1 - (P_{1,L-1,0} + P_{1,L-1,1} + P_{0,L,0} + P_{0,L,1}) = 1 - P_{L-1}\begin{bmatrix}0\\1\\0\\1\end{bmatrix} - P_L\begin{bmatrix}1\\1\end{bmatrix}. \tag{8}$$

3.2. Reliability function

In this section, under the condition that at time $t = 0$ all system components are operational and new, our objective is to determine the system reliability $R(t)$ and the time to first failure $MTTF$. In order to achieve this, we modify the model by making the failure states $(0, L, 1)$, $(0, L, 0)$, $(1, L-1, 0)$ and $(1, L-1, 1)$ absorbing states (i.e., removing all transitions from these states to functioning states). This results in a new $CTMC$ $\{\tilde{X}(t), t \geq 0\}$, with state space $\tilde{E} = \{(i, j, n), 0 \leq i \leq 1, , 0 \leq j \leq L-2, 0 \leq n \leq 1\} \cup \{(0, L, 1)\}$. Its generator matrix $\tilde{Q}$ of order $4L + 1 \times 4L + 1$ is defined by:

$$\tilde{Q} = \begin{pmatrix} B_0 & C_0 & & & & \\ A & B_1 & C_1 & & & \\ & A & B_2 & C_2 & & \\ & & \ddots & \ddots & \ddots & \\ & & & A & \tilde{B}_{L-1} & \tilde{C}_L \\ & & & & & 0 \end{pmatrix}_{4L+1\times 4L+1},$$

where

$$\tilde{B}_{L-1} = \begin{bmatrix} -(\eta_{L-1}+\theta+\gamma) & -\eta_{L-1} & \theta & 0 \\ 0 & 0 & 0 & 0 \\ \sigma & 0 & -\sigma & 0 \\ 0 & 0 & 0 & 0 \end{bmatrix}, \quad \text{and} \quad \tilde{C}_L = \begin{bmatrix} 0 \\ 0 \\ \eta_{L-1} \\ 0 \end{bmatrix}.$$

The state-transition diagram of $\{\tilde{X}(t), t \geq 0\}$ is shown in Figure 4.

Let $P(t) = (P_0(t), P_1(t), \ldots, P_{L-1}(t), P_L(t))$ be the state probability vector of $\{\tilde{X}(t), t \geq 0\}$, where $P_j(t) = (P_{0,j,0}(t), P_{1,j,0}(t), P_{0,j,1}(t), P_{1,j,1}(t))$ $(j = 0, 1, \ldots, L-1)$ and $P_L = P_{0,L,1}(t)$. The vector $P(t)$ can be obtained by solving the differential matrix equation:

$$\frac{dP(t)}{dt} = P(t).\tilde{Q}, \tag{9}$$

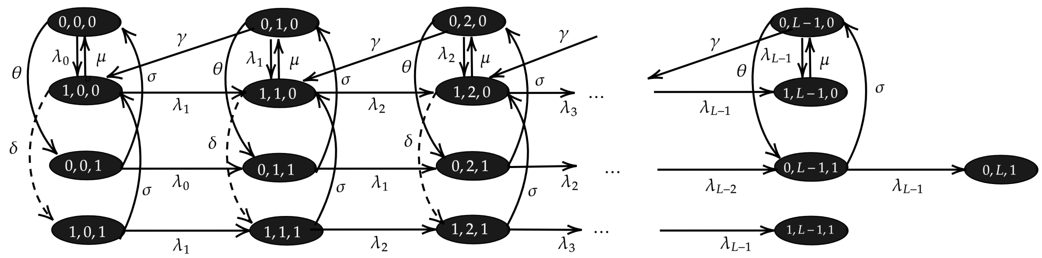

Figure 4: *State-transition diagram of* $\{\tilde{X}(t), t \geq 0\}$

together with $P(t).e = 1$, where $e = (1, 1,\ldots, 1)^t$ is a unit vector with dimension $4L + 1$ and $\frac{dP(t)}{dt} = (\frac{dP_0(t)}{dt}, \frac{dP_1(t)}{dt}(t), \ldots, \frac{dP_{L-1}(t)}{dt}, \frac{dP_L(t)}{dt})$, with

$$\frac{dP_j(t)}{dt} = \begin{cases} \left(\frac{dP_{0,j,0}(t)}{dt}, \frac{dP_{1,j,0}(t)}{dt}, \frac{dP_{0,j,1}(t)}{dt}, \frac{dP_{1,j,1}(t)}{dt}\right), & \text{for } j = 0, 1, \ldots, L-1, \\ \frac{dP_{0,L,1}(t)}{dt}, & \text{for } j = L. \end{cases}$$

Applying the Laplace transform to both sides of equation (9), we get:

$$P^*(s)(sI - \tilde{Q}) = P(0), \tag{10}$$

where the initial row vector $P(0)$ is given by $P(0) = (1, 0, 0, 0, 0, \ldots, 0)$ and $P^*(s) = (P_0^*(s), P_1^*(s), \ldots, P_{L-1}^*(s), P_L^*(s))$ with $P_j^*(s) = (P_{0,j,0}^*(s), P_{1,j,0}^*(s), P_{0,j,1}^*(s), P_{1,j,1}^*(s))$ $(j = 0, 1, \ldots, L-1)$, $P_L^* = P_{0,L,1}(s)$ and $P_{i,j,n}^*(s) = \int_0^{+\infty} e^{-st} P_{i,j,n}(t)\, dt$.

Solving equation (10) is a complex task that requires advanced computational techniques. In this study, we leverage Matlab software to facilitate the solution process. Specifically, by applying the inverse Laplace transform to $P_{1,L-1,0}^*(s)$, $P_{1,L-1,1}^*(s)$ and $P_{0,L,1}^*(s)$, we obtain the expression for $P_{1,L-1,0}(t)$, $P_{1,L-1,1}(t)$ and $P_{0,L,1}(t)$, which gives the probability that the system fails at or before time t, given that the repairer is occupied. The inverse Laplace transform is computed numerically using the algorithm presented below:

Algorithm 1 Laplace Inverse Transform Computation of $P_{1,L-1,0}^*(s)$, $P_{1,L-1,1}^*(s)$, and $P_{0,L,1}^*(s)$

1. Construct the generator matrix $\tilde{Q}$.
2. Compute $q(s) = sI - \tilde{Q}$.
3. Calculate the matrix $A(s) = [sI - Q]^{-1}$ by matrix inversion.
4. Determine the Laplace transform of state probabilities $P^*(s) = P(0) \cdot A(s)$.
5. Calculate the inverse Laplace transforms of $P_{1,L-1,0}^*(s)$, $P_{1,L-1,1}^*(s)$, and $P_{0,L,1}^*(s)$ using the symbolic `ilaplace` function in MATLAB, to obtain the expressions for $P_{1,L-1,0}(t)$, $P_{1,L-1,1}(t)$, and $P_{0,L,1}(t)$.

Let $R(t)$ be the reliability function of the system, then $R(t)$ is given by:

$$R(t) = 1 - P_{1,L-1,0}(t) - P_{1,L-1,1}(t) - P_{0,L,1}(t). \tag{11}$$

To find the mean time to the first failure ($MTTF$) we use the following formula:

$$MTTF = \int_0^{+\infty} R(t)\, dt. \tag{12}$$

4. Numerical example

In this section, we study the sensitivity of the system Availability A_∞, reliability $R(t)$ and the mean time to the first failure $MTTF$ with respect to system parameters. This analysis is based on a base case with the following parameter values: $\mu = 2$, $\eta = 0.6$, $\sigma = 1$, $\alpha = 0.05$, $\delta = 0.8$, $\theta = 0.5$ and $\gamma = 3$, $M = 3$, $W = 2$, $C = 1$, $K = 2$. The resulting numerical values for $A(\infty)$ and $R(t)$ are illustrated in figures 5-6 and 7-9, respectively.

Figures 5-9 illustrate that both A_∞ and $R(t)$ exhibit similar behavior with respect to all parameters. Specifically, A_∞ and $R(t)$ increase as μ, γ, and σ rise, while they decrease with higher values of η and δ. The impact of θ is also evident in reducing A_∞, though its effect on $R(t)$ remains negligible. However, the parameter α has little to no influence on either A_∞ or $R(t)$.

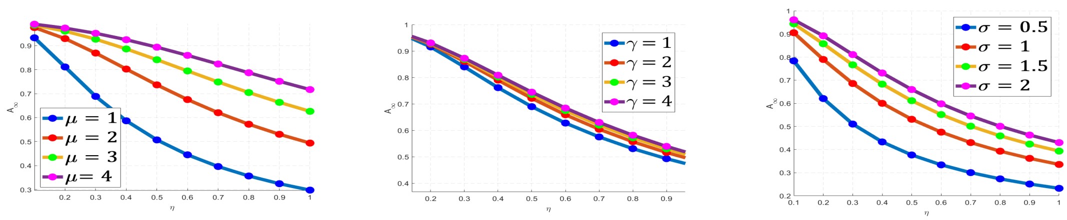

(a) A_∞ vs η for μ (b) A_∞ vs η for γ (c) A_∞ vs η for σ

Figure 5: *Steady-state availability A_∞ vs system parameters μ, γ, and σ.*

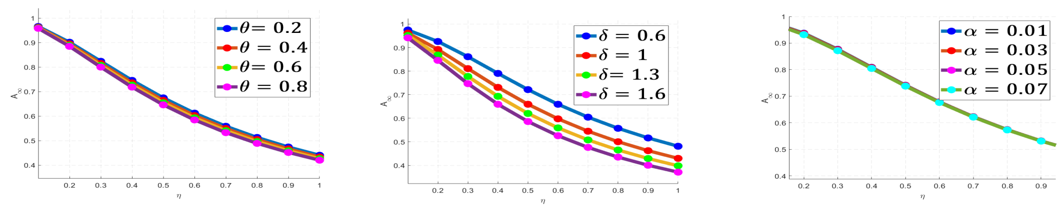

(a) A_∞ vs η for θ (b) A_∞ vs η for δ (c) A_∞ vs η for α

Figure 6: *Steady-state availability A_∞ vs system parameters θ, δ, and α.*

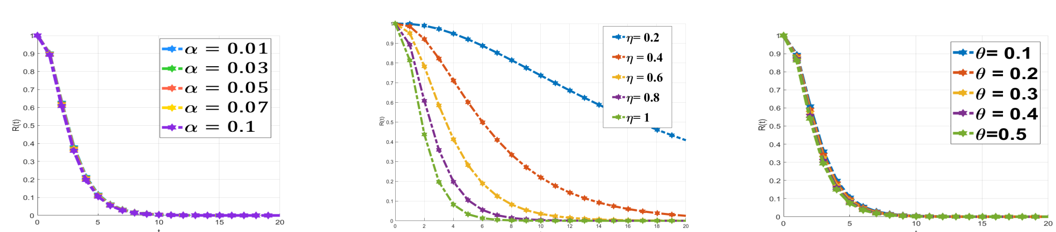

(a) $R(t)$ vs α (b) $R(t)$ vs η (c) $R(t)$ vs θ

Figure 7: *Reliability function $R(t)$ vs system parameters α, η, and θ.*

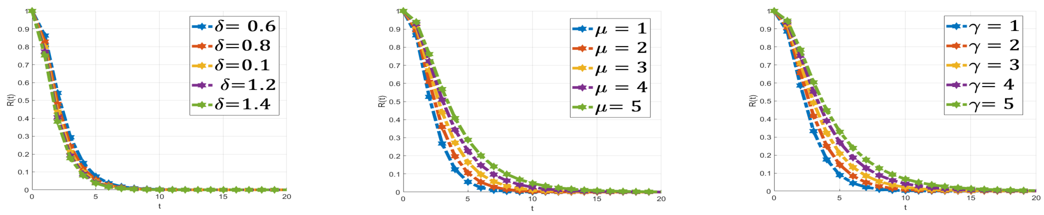

(a) $R(t)$ vs δ (b) $R(t)$ vs μ (c) $R(t)$ vs γ

Figure 8: *Reliability function $R(t)$ vs system parameters δ, μ, and γ.*

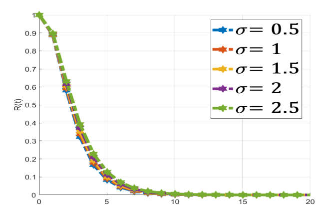

Figure 9: *Reliability function $R(t)$ vs system parameter σ.*

Tables 4-9, show the impact of system parameters (α, δ, θ, μ, γ and σ) on the Mean Time to First Failure ($MTTF$) across various values of η.

From Tables 4-9, we observe that when η increases $MTTF$ decreases.

• **MTTF versus α and η**: As α increases, $MTTF$ consistently decreases for all values of η. In other words, systems with higher α values are more susceptible to failure, particularly when the system experiences higher arrival rates η.

η	0.1	0.2	0.6	0.8	1
$\alpha = 0.01$	140.1234	31.5767	5.1234	3.2098	2.4895
$\alpha = 0.03$	128.4567	30.2094	5.0672	3.1465	2.4672
$\alpha = 0.05$	118.4785	28.9012	5.0128	3.0869	2.4451
$\alpha = 0.07$	110.3476	27.7215	4.9602	3.0293	2.4234
$\alpha = 0.09$	102.5963	26.5954	4.9085	2.9746	2.4020

Table 4: *$MTTF$ versus α and η*

• **MTTF versus δ and η**: As δ increases, the $MTTF$ decreases across all values of η. This indicates that higher values of δ result in a shorter mean time to first failure.

η	0.1	0.2	0.6	0.8	1
$\delta = 0.5$	111.5089	28.1384	4.4212	2.8441	2.0396
$\delta = 0.8$	58.5872	18.5609	3.6766	2.4770	1.8323
$\delta = 1$	39.4558	14.1038	3.2244	2.2372	1.6890
$\delta = 1.5$	30.0999	11.6221	2.9228	2.0688	1.5842
$\delta = 2$	24.7013	10.0700	2.7082	1.9443	1.5042

Table 5: *$MTTF$ versus δ and η*

• **MTTF versus θ and η**: Similar to δ, increasing θ leads to a decrease in $MTTF$.

η	0.1	0.2	0.6	0.8	1
$\theta = 0.2$	167.8474	38.1113	4.8983	3.0468	2.1423
$\theta = 0.4$	111.5089	28.1384	4.4212	2.8441	2.0396
$\theta = 0.6$	80.1144	22.0062	4.0379	2.6730	1.9502
$\theta = 0.8$	62.2545	18.1904	3.7331	2.5294	1.8725
$\theta = 1$	51.2662	15.6842	3.4895	2.4087	1.8050

Table 6: $MTTF$ *versus* θ *and* η

• **MTTF versus μ and η**: Increasing μ, results in a noticeable increase in $MTTF$. Higher μ values enhance system durability and reduce the probability of early failures. This effect is consistent across all stress levels η.

η	0.1	0.2	0.6	0.8	1
$\mu = 1$	33.3047	10.8693	2.4141	1.6881	1.2885
$\mu = 2$	69.9236	19.0933	3.3649	2.2354	1.6440
$\mu = 3$	111.5089	28.1384	4.4212	2.8441	2.0396
$\mu = 4$	153.9382	37.3126	5.5455	3.4970	2.4656
$\mu = 5$	194.8966	46.2035	6.7106	4.1810	2.9147

Table 7: $MTTF$ *versus* μ *and* η

• **MTTF versus γ and η**: Increasing γ significantly boosts $MTTF$. The effect becomes more significant as η increases.

η	0.1	0.2	0.6	0.8	1
$\gamma = 1$	111.5089	28.1384	4.4212	2.8441	2.0396
$\gamma = 2$	198.7491	35.8419	4.6921	2.9510	2.0892
$\gamma = 3$	307.7273	41.2081	4.8511	3.0153	2.1201
$\gamma = 4$	452.1257	45.2651	4.9574	3.0588	2.1414
$\gamma = 5$	655.2260	48.4745	5.0343	3.0904	2.1571

Table 8: $MTTF$ *versus* γ *and* η

• **MTTF versus σ and η**: As σ increases, $MTTF$ also increases. This effect holds at all values of η.

η	0.1	0.2	0.6	0.8	1
$\sigma = 1$	111.5089	28.1384	4.4212	2.8441	2.0396
$\sigma = 1.5$	174.9496	38.6161	4.8138	2.9923	2.1063
$\sigma = 2$	195.1836	42.9104	5.0091	3.0707	2.1435
$\sigma = 2.5$	202.6555	44.9603	5.1208	3.1177	2.1667
$\sigma = 3$	205.9744	46.0936	5.1916	3.1485	2.1824

Table 9: $MTTF$ *versus* σ *and* η

4.1. Model Validation through Simulation

To support the analytical results, we conducted a simulation using TimeNET 5.0.1 and included comparative plots of both the steady-state availability A_∞ and the reliability function $R(t)$ (see Figures 10-11), which confirm the accuracy and consistency of the proposed model.

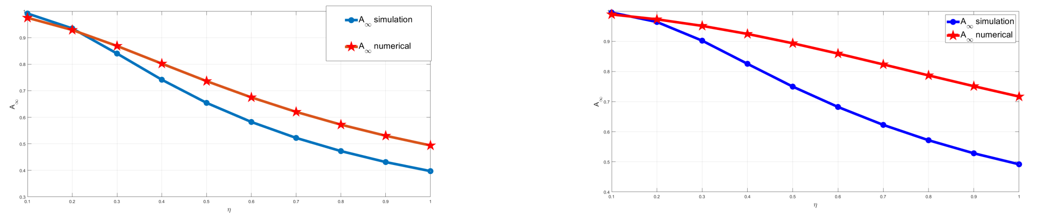

(a) A_∞ *vs* η *for* $\mu = 2$, $\eta = 0.6$, $\sigma = 1$, $\alpha = 0.05$, $\delta = 0.8$, $\theta = 0.5$, *and* $\gamma = 3$

(b) A_∞ *vs* η *for* $\mu = 4$, $\eta = 0.6$, $\sigma = 1$, $\alpha = 0.05$, $\delta = 0.8$, $\theta = 0.5$, *and* $\gamma = 3$

Figure 10: *Analytical vs simulated steady-state availability* A_∞.

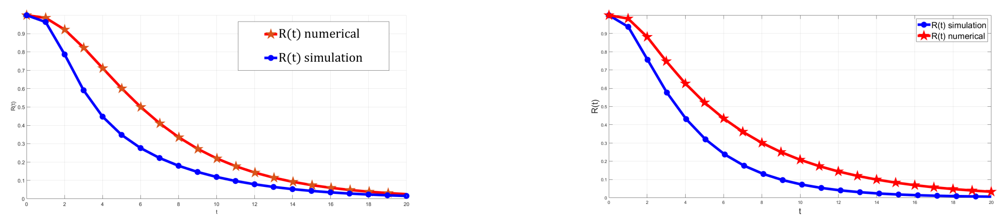

(a) $R(t)$ *vs* t *for* $\mu = 2$, $\eta = 0.6$, $\sigma = 1$, $\alpha = 0.05$, $\delta = 0.8$, $\theta = 0.5$, *and* $\gamma = 3$

(b) $R(t)$ *vs* t *for* $\mu = 4$, $\eta = 0.6$, $\sigma = 1$, $\alpha = 0.05$, $\delta = 0.8$, $\theta = 0.5$, *and* $\gamma = 3$

Figure 11: *Analytical vs simulated reliability function* $R(t)$.

Based on Figures 10-11, the numerical method consistently achieves higher values of $R(t)$ over time, indicating superior reliability performance across the operational period. It also yields smoother reliability curves and higher asymptotic availability $A(\infty)$, reflecting enhanced long-term system dependability. Although simulation methods are advantageous for systems with large state spaces due to their flexibility and computational efficiency, in this case, the numerical approach proves more effective in preserving reliability and delivering robust performance.

5. Conclusion

This paper employed a $GSPN$-based model to assess the reliability and performance of a retrial K-out-of-n system that incorporates cold and warm standbys and an unreliable repairer. A finite-state $CTMC$ is derived from the $GSPN$ model. Then we determined the steady-state availability by resolving the steady-state probability equations in matrix form. Using the Laplace transform method, we obtained the main reliability indices in the transient state. Numerical examples illustrated the sensitivity analysis of reliability indices regarding the parameters of the system. Future work will focus on extending the current model in several key directions. First, we plan to explore Markov Regenerative Stochastic Petri Nets (MRSPNs) to represent systems with general lifetime or repair time distributions. This framework relaxes the exponential time assumption and is expected to yield more accurate evaluations of system reliability and availability, particularly in complex redundant architectures. In addition, we aim to address the commonly made assumption of statistical independence among failures, repairs, and retrials. In many real-world systems, such events are interdependent—failure rates may depend on workload, and repair durations may be correlated. Incorporating these dependencies will enhance the model's realism and applicability to practical scenarios. Finally, future developments will consider weighted k-out-of-n systems, where certain components contribute more critically to overall system function. This extension will enable the model to better reflect scenarios in which components play unequal roles, providing a more nuanced and realistic characterization of system behavior.

References

[1] Amari, S. V. (2012). Reliability of k-out-of-n standby systems with Gamma distributions. In: *Proceedings of the 2012 Annual Reliability and Maintainability Symposium (RAMS)*, 1–6. doi: 10.1109/RAMS.2012.6175471

[2] Ajmone Marsan, M., Balbo, G., Conte, G., Donatelli, S., and Franceschinis, G. (1995). Modelling with Generalized Stochastic Petri Nets. New York: John Wiley & Sons.

[3] Barlow, R.E. and Proschan, F. (1975) *Statistical Theory of Reliability and Life Testing.* New York: Holt, Rinehart and Winston.

[4] Birolini, A. (2010). Reliability Engineering: Theory and Practice. Springer.

[5] Oliveira, C. A. L., and Lima, M. F. (2009). Performance analysis of resource-constrained business processes: A formal approach based on stochastic Petri nets. *Technical Report*, Centro de Informática, Universidade Federal de Pernambuco, March 2009. url: https://www.cin.ufpe.br/ calo/publications/Oliveira09%20-%20Performance%20Analysis%20of%20Business%20Processes%20(tech-report).pdf

[6] Gharbi, N., and Charabi, L. (2012). Wireless networks with retrials and heterogeneous servers: Comparing random server and fastest free server disciplines. International Journal on Advances in Networks and Services, 5, 102-115.

[7] Gharbi, N., and Dutheillet, C. (2011). An algorithmic approach for analysis of finite-source retrial systems with unreliable servers. Computers and Mathematics with Applications, 62, 2535-2546. doi: 10.1016/j.camwa.2011.03.109

[8] Gharbi, N., and Ioualalen, M. (2010). Numerical investigation of finite-source multiserver systems with different vacation policies. Journal of Computational and Applied Mathematics, 234, 625-635. doi: 10.1016/j.cam.2009.11.040

[9] Gharbi, N., Nemmouchi, B., Mokdad, L., and Ben-Othman, J. (2014). The impact of breakdown disciplines and repeated attempts on performances of small cell networks. Journal of Computational Science, 5(4), 633-644. doi: 10.1016/j.jocs.2014.02.011

[10] Hakmi, S., Lekadir, O., and Aïssani, D. (2019). Analysis of priority queue with repeated attempts using generalized stochastic Petri nets. Miskolc Mathematical Notes, 20, 925-939. doi: 10.18514/MMN.2019.2620

[11] Hu, H., Yu, J., Li, Z., Chen, J., and Hu, H. (2021). Modeling and analysis of cyber–physical system based on object-oriented generalized stochastic Petri net. IEEE Transactions on Reliability, 70(3), 1186-1199. doi: 10.1109/TR.2020.2998091

[12] Kant, S., Kant, S., Yadav, M., Chaukiyal, A., and Jamwal, B. (2024). Profit analysis of repairable warm standby system. Reliability: Theory & Applications, 4(80), 461-467. url: https://gnedenko.net/Journal/2024/042024/RTA_4_2024-38.pdf

[13] Ke, J. C., and Wang, K. H. (2002). The reliability analysis of balking and reneging in a repairable system with warm standbys. Quality and Reliability Engineering International, 18, 467-478. doi: 10.1002/qre.495

[14] Ke, J. C., Yang, D. Y., Sheu, S. H., and Kuo, C.-C. (2013). Availability of a repairable retrial system with warm standby components. International Journal of Computer Mathematics, 90(11), 2279-2297. doi: 10.1080/00207160.2013.783695

[15] Kececioglu, D. (2002). *Reliability Engineering Handbook.* DEStech Publications, Inc.

[16] Kuo, C. C., Sheu, S. H., Ke, J. C., and Zhang, Z.-G. (2014). Reliability-based measures for a retrial system with mixed standby components. Applied Mathematical Modelling, 38(19-20), 4640-4651. doi: 10.1016/j.apm.2014.03.005

[17] Lai, C-D., and Xie, M. (2006). *Stochastic Ageing and Dependence for Reliability.* New York, NY: Springer. doi: 10.1007/0-387-34232-X

[18] Levitin, G., and Amari, S. V. (2010). Approximation algorithm for evaluating time-to-failure distribution of k-out-of-n system with shared standby elements. Reliability Engineering and System Safety, 95, 396-401. doi: 10.1016/j.ress.2009.11.010

[19] Liu, S., Li, W., Gao, P., and Sun, Y. (2022). Modeling and performance analysis of gas leakage emergency disposal process in gas transmission station based on Stochastic Petri nets. Reliability Engineering & System Safety, 226, 108708. doi: 10.1016/j.ress.2022.10870

[20] Smith, D., J. (2011). *Reliability, Maintainability and Risk*. Butterworth-Heinemann. doi: 10.1016/C2010-0-66333-4

[21] Srinivas, R. C., Krishnamoorthy, A., and Ushakumari, P. V. (2001). A k-out-of-n reliability system with an unreliable server and phase-type repairs and services: The (N,T) policy. Journal of Applied Mathematics and Stochastic Analysis, 14(4), 361-380. doi: 10.1155/S1048953301000326

[22] Unuvar, M., Ozguven, E. E., and Prékopa, A. (2020). Optimal capacity design under k-out-of-n and consecutive k-out-of-n type probabilistic constraints. Annals of Operations Research, 226, 643-657. doi: 10.1007/s10479-014-1712-5

[23] Viswanadham, S., Narahari, Y., and Johnson, L. (1990). Deadlock prevention and deadlock avoidance in flexible manufacturing systems using Petri net models. Transactions on Robotics and Automation, 6(6). doi: 10.1109/70.63257

[24] Wang, W., and Loman, J. (2002). Reliability/Availability of K-out-of-N System with M Cold Standby Units. In: *IEEE 2002 Proceedings Annual Reliability and Maintainability Symposium*. doi: 10.1109/RAMS.2002.981684

[25] Yuan, L. (2021). Reliability analysis for a k-out-of-n: G system with redundant dependency and repairmen having multiple vacations. Applied Mathematics and Computation, 218, 11959-11969. doi: 10.1016/j.amc.2012.06.006

[26] Yadollahzadeh Tabari, M., and Mohammadizad, P. (2020). Modeling and performance evaluation of energy consumption in S-MAC protocol using generalized stochastic Petri nets. International Journal of Engineering, 33(6), 1114-1121. doi: 10.5829/ije.2020.33.06c.08

[27] Yadollahzadeh-Tabari, M. (2021) An stochastic reward net model for performance analysis of network layer in mobile ad hoc network under the workload of misbehavior nodes. Wireless Personal Communications, 118, 1087–1109. doi: 10.1007/s11277-020-08060-0

[28] Yadollahzadeh-Tabari, M., Pouyan, A. A. (2017) Misbehavior analysis of IEEE 802.11 MAC layer in mobile ad hoc network using stochastic reward nets. International Journal of Communication Systems, 30(17), e3385. doi: 10.1002/dac.3385

[29] Pouyan, A., Yadollahzadeh-Tabari, M. (2014) Estimating reliability in mobile ad-hoc networks based on Monte Carlo simulation. International Journal of Engineering (IJE), IJE Transactions B: Applications, 27(5), 739–746. url: https://www.ije.ir/article$_7$2305*.html*

[30] Zeng, Y., Duan, R., Huang, S., and Feng, T. (2020). Reliability analysis for complex systems based on generalized stochastic Petri nets and EDA approach considering common cause failure. Engineering Computations, 37, 1513-1530. doi: 10.1108/EC-05-2019-0241